

Two-point function of strangeness-carrying vector-currents in two-loop Chiral Perturbation Theory

Stephan Dürr^{*a,b} and Joachim Kambor^{†c}

^a*University of Washington, Physics Department, Seattle, WA 98195-1560, U.S.A.*

^b*Paul Scherrer Institute, Particle Theory Group, 5232 Villigen, Switzerland*

^c*University of Zürich, Institute for Theoretical Physics, 8057 Zürich, Switzerland*

Abstract

We calculate the correlator between two external vector-currents having the quantum-numbers of a charged kaon. We give the renormalized expression to two loops in standard chiral perturbation theory in the isospin limit, which, as a physical result, is finite and scale-independent. Applications include a low energy theorem, valid at two loop order, of a flavor breaking combination of vector current correlators as well as a determination of the phenomenologically relevant finite $O(p^6)$ -counterterm combination Q_V by means of inverse moment finite energy sum rules. This determination is less sensitive to isospin-breaking effects than previous attempts.

Preprint numbers: UW-PT/99-14, ZU-TH/15-98, hep-ph/9907539

PACS numbers: 12.39.Fe, 11.55.Hx

*stephan.duerr@psi.ch

†kambor@physik.unizh.ch

I. INTRODUCTION

The appropriate tool to analyze hadronic processes at very low energies is chiral perturbation theory (XPT), the low energy effective theory of QCD. The general structure of XPT is well understood [1–4], and it has been successfully applied at the one- and two-loop level to a vast body of low-energy data. Recently, the non-anomalous counterterm Lagrangian at $O(p^6)$ has been constructed in full generality for chiral $SU(N)$ [5], thereby closing a gap left behind in an earlier attempt [6]. The divergent part of the generating functional at the two-loop level has also been calculated in closed form and is now available [7].

Despite this advanced state on the theoretical side, phenomenological applications at the two-loop level are relatively scarce [8–10]. Two reasons may be responsible for this shortcoming: being an effective theory, XPT introduces new, unknown coupling constants at each order of the perturbation series. The number of such unknown parameters is rather large at $O(p^6)$ [5]. Consequently, it is a priori not clear whether at this order independent physical processes can be related in a parameter free manner – at one-loop one of the main virtues of XPT. The second, more technical reason, is the large computational effort demanded to perform complete two-loop calculations, comprising the finite contributions to loop-integrals and counterterms, in particular in the 3-flavor case.

In this paper we calculate the two-point function of strangeness carrying vector currents to $O(p^6)$ in standard XPT. Although completely analogous to the calculation of the correlator of flavor diagonal currents considered in [9], the non-equal masses propagating in the loops make the present investigation technically more demanding. We use a method where one-loop subgraphs are renormalized before the second loop-integration is performed, which helps simplifying intermediate expressions. Combining our result with the isospin and hypercharge component of the vector correlator obtained in [9], we can form a “low energy theorem”, i.e. a *parameter free* relation between physical quantities, valid at $O(p^6)$. This shows that, despite the many coupling constants present at this order, there are still specific flavor breaking combinations of observables which can be predicted in terms of meson masses and decay constants only.

A more phenomenological motivation of the present calculation derives from experimental efforts to determine the spectral functions of strangeness carrying currents. The ALEPH collaboration has recently published their analysis of τ -decays into hadronic final states with strangeness [11]. This concatenation of data allows to connect, via inverse moment finite energy sum rules (IMFESR), the vector current correlator at low energies calculated in this paper to the asymptotic behavior of the correlator obtained by the operator product expansion [12]. As a result, we are able to fix a coupling constant of the $O(p^6)$ chiral Lagrangian, Q_V , from the difference of isovector and strange component of the vector spectral functions. The constant Q_V has been estimated in Ref. [13] from the difference of isovector and hypercharge components of the vector spectral functions. However, as pointed out in [14], that determination is sensitive to isospin violating corrections affecting mainly the hypercharge current. The strange current on the other hand is not sensitive to isospin violation, and the determination of Q_V presented in this paper is therefore more reliable.

The article is organized as follows. Section II contains an outline of the general strategy employed in the calculation and a derivation of the strange formfactor which plays a central role in it. In Section III the two-point correlator $\langle T\{V_s V_s^\dagger\} \rangle$ between two strangeness carrying

external vector-currents is derived. The physical content of this result is discussed in Section IV where we also point out several consistency checks. Combining strange, isospin and hypercharge component of the vector two-point function yields a new low energy theorem valid at $O(p^6)$. In section V we present a determination of the low energy constant Q_V by employing an inverse moment finite energy sum rule for the difference of isovector and strange component of the vector current spectral functions. Finally, section VI contains our conclusions. Some technical details are collected in the Appendix.

II. FORM FACTOR CALCULATION AND DESCRIPTION OF THE METHOD

For explicit calculations we shall use the Lagrangian of standard XPT

$$\mathcal{L} = \mathcal{L}^{(2)} + \mathcal{L}^{(4)} + \mathcal{L}^{(6)} \quad (1)$$

where $\mathcal{L}^{(i)}$ denotes the Lagrangian of order p^i . The first two terms in this expansion can be found in the work by Gasser and Leutwyler [3,4] which also discusses how the meson fields couple to external sources. The last term, i.e. the one of order p^6 , has recently been constructed for the non-anomalous sector in [5], thereby reducing the older form given in [6] to a minimal set. We shall employ the SU(3) version of the Lagrangian given in [5].

From (1), the correlation function between two external vector currents with the quantum numbers of a kaon could be computed following the usual procedure: Draw all Feynman diagrams contributing at $O(p^4)$ and $O(p^6)$ in standard XPT [2,3] (see Fig. 1 and Fig. 2), evaluate them and have the divergences in the loop- and counterterm-contributions canceled to get the finite physical result valid in 4 dimensions. Naively following this recipe would amount to compute the two-loop integrals in terms of unrenormalized masses and couplings. As it turns out, the two-loop contributions are significantly shorter if they are expressed in terms of one-loop renormalized expressions.

A well known method to do this is simply combining diagrams (e) and (f) in Fig. 2 into a new single diagram, equivalent in topology to the one-loop unitary diagram, employing mass- and wavefunction-renormalization correct to $O(p^4)$. Likewise, diagrams (b) and (c) can be replaced by a single new diagram, topologically equivalent to the one-loop tadpole-diagram, without altering the expression at $O(p^6)$, if one-loop masses are used. In the remaining six diagrams in Fig. 2, the K, π, η -masses may be taken as the one-loop renormalized masses as well, since the corresponding change shows up at $O(p^8)$ only.

An alternative method uses the strategy of renormalizing intermediate results in an even more direct, physical way. It is known as the “master method” and was introduced in the context of XPT in ref. [10]. The idea is to start from the one-loop expression for the formfactor of the strangeness-carrying vector-current with any of the possible intermediate particle-combinations of the VV -correlator in the final state. The correlator follows by contracting this formfactor with its hermitian conjugate (modulo a modification necessary to avoid double-counting, c.f. Sec. III), integrating over internal momenta, adding tadpole- and counterterm-contributions and completing the remaining renormalization procedure.

We have calculated $\langle T\{V_s V_s^\dagger\} \rangle$ following either one of these two methods and have found the results to agree. For this reason we restrict ourselves to presenting the calculation in

the second, more physical framework. Below we summarize the results for the strangeness-carrying formfactor, while section III contains the derivation of the correlator.

It is clear that the technical key quantity needed in the second strategy is the *off-shell* form-factor $S_\mu[P_1 P_2](p_1, p_2)$, i.e. the amplitude for an external vector-current with momentum $q_\mu = (p_1 + p_2)_\mu$ and the quantum numbers of a K^+ to decay into any of the combinations $P_1 P_2 = (K^+ \pi^0, K^+ \eta, K^0 \pi^+)$ with *arbitrary* momenta p_1 and p_2 , respectively. Note that S_μ is not a physical quantity, i.e. the result depends on the choice of interpolating fields for the Goldstone bosons. However, the correlator we are aiming at involves an integration over these fields and is independent of this choice. For convenience, the formfactor shall be separated into a symmetric and an antisymmetric piece w.r.t. the outgoing momenta

$$S_\mu[P_1 P_2] = S_+[P_1 P_2](p_1 + p_2)_\mu + S_-[P_1 P_2](p_1 - p_2)_\mu \quad (2)$$

and the convention is that p_1 denotes the momentum of the strange meson ($P_1 = K^+, K^0$), whereas p_2 is the momentum of the non-strange meson ($P_2 = \pi^0, \eta, \pi^+$). Fig. 3 displays diagrammatically the relevant contributions. Diagram (a) represents the leading $O(p^2)$ -contribution, whereas diagrams (b, c) as well as (d, e, f) are of order $O(p^4)$. The latter three are frequently referred to as the “unitary”-, “tadpole”- and “counterterm”-contributions. The sum of these six diagrams corresponds to a single formfactor-diagram in the effective theory [in the field-theoretic sense, i.e. in the theory where all quantum corrections have been absorbed into the propagators and vertices of the effective action and Greens functions are constructed from tree-level diagrams only] where the two outgoing mesons carry the full wavefunction-renormalization factors Z_{P_1}, Z_{P_2} , with $Z_P = 1 - A_P$ and

$$A_\pi = \frac{i}{F_0^2} \left(-\frac{2}{3} A(M_\pi^2) - \frac{1}{3} A(M_K^2) \right) + \frac{8}{F_0^2} \left((2M_K^2 + M_\pi^2) L_4 + M_\pi^2 L_5 \right) \quad (3)$$

$$A_K = \frac{i}{F_0^2} \left(-\frac{1}{4} A(M_\pi^2) - \frac{1}{2} A(M_K^2) - \frac{1}{4} A(M_\eta^2) \right) + \frac{8}{F_0^2} \left((2M_K^2 + M_\pi^2) L_4 + M_K^2 L_5 \right) \quad (4)$$

$$A_\eta = \frac{i}{F_0^2} \left(-A(M_K^2) \right) + \frac{8}{F_0^2} \left((2M_K^2 + M_\pi^2) L_4 + M_\eta^2 L_5 \right). \quad (5)$$

However, in the light of the application to follow, it is extremely convenient to have the external legs carry a factor $\sqrt{Z_P}$, rather than Z_P or 1. Since $Z_P = 1 - A_P$ implies $\sqrt{Z_P} = 1 - \frac{1}{2} A_P + O(p^4)$ and since we are interested in S_μ to $O(p^4)$, this “ $\sqrt{Z_P}$ -convention” amounts to defining $S_\mu[P_1 P_2]$ as a weighted sum: Diagrams (a, d, e, f) are included with their full weight, but diagrams (b, c) with a factor $\frac{1}{2}$ only. Note that renormalizability of the on-shell formfactor is not affected by such a reweighting as long as diagrams (b) and (c) receive the same factor and the group (d, e, f) also receives a common factor. In practice, on-shell renormalizability is implemented as follows: First replace $p_1^2 \rightarrow M_K^2$, $p_2^2 \rightarrow M_{P_2}^2$ ($P_2 = \pi^+, \pi^0, \eta$), where M_P denotes the *one-loop* mass of particle P . Next, expand all integrals in $1/(d-4)$, or equivalently in $\bar{\lambda}$, as is explained in the Appendix, and simultaneously the renormalization constants according to

$$L_i \rightarrow \mu^{d-4} \cdot (L_i^{(1)} \bar{\lambda} + L_i^{(0)} + O(\bar{\lambda}^{-1})). \quad (6)$$

Finally, check that there is indeed a set of numerical constants $\{L_i^{(1)}\}$ for which all contributions in $\bar{\lambda}$ cancel exactly. These “divergent” parts of the one-loop counterterms agree of course with their standard values $L_i^{(1)} = \Gamma_i$ [2,3].

In summary, the strange *off-shell* formfactor takes the form (2) with

$$\begin{aligned}
S_+[K^+\pi^0] = \frac{1}{F_0^2} \left\{ -\frac{1}{16} [-5A_{\text{fin}}(M_\pi^2) + 2A_{\text{fin}}(M_K^2) + 3A_{\text{fin}}(M_\eta^2)] \right. \\
-2i L_5^{(0)}(M_K^2 - M_\pi^2) + i L_9^{(0)}(p_1^2 - p_2^2) \\
+\frac{1}{48} [M_K^2 + M_\pi^2 + 5(p_1^2 + p_2^2 - 3q^2)] \frac{M_K^2 - M_\pi^2}{q^2} \overline{B}(q^2, M_K^2, M_\pi^2) \\
-\frac{1}{48} [3M_K^2 + 3M_\pi^2 + 3(p_1^2 + p_2^2 - 3q^2)] \frac{M_K^2 - M_\eta^2}{q^2} \overline{B}(q^2, M_K^2, M_\eta^2) \\
\left. +\frac{3}{16} \frac{p_1^2 - p_2^2}{q^2} [(T_{\text{fin}}^{(0)} - T_{\text{fin}}^{(1)})(q^2, M_K^2, M_\pi^2) + (T_{\text{fin}}^{(0)} - T_{\text{fin}}^{(1)})(q^2, M_K^2, M_\eta^2)] \right\} \quad (7)
\end{aligned}$$

$$\begin{aligned}
S_+[K^+\eta] = \frac{\sqrt{3}}{F_0^2} \left\{ -\frac{3}{16} [A_{\text{fin}}(M_\pi^2) - 2A_{\text{fin}}(M_K^2) + A_{\text{fin}}(M_\eta^2)] \right. \\
-2i L_5^{(0)}(M_K^2 - M_\eta^2) + i L_9^{(0)}(p_1^2 - p_2^2) \\
+\frac{1}{48} [M_K^2 - 7M_\pi^2 - 3(p_1^2 + p_2^2 - 3q^2)] \frac{M_K^2 - M_\pi^2}{q^2} \overline{B}(q^2, M_K^2, M_\pi^2) \\
-\frac{1}{48} [19M_K^2 - 5M_\pi^2 + 3(p_1^2 + p_2^2 - 3q^2)] \frac{M_K^2 - M_\eta^2}{q^2} \overline{B}(q^2, M_K^2, M_\eta^2) \\
\left. +\frac{3}{16} \frac{p_1^2 - p_2^2}{q^2} [(T_{\text{fin}}^{(0)} - T_{\text{fin}}^{(1)})(q^2, M_K^2, M_\pi^2) + (T_{\text{fin}}^{(0)} - T_{\text{fin}}^{(1)})(q^2, M_K^2, M_\eta^2)] \right\} \quad (8)
\end{aligned}$$

$$S_+[K^0\pi^+] = \sqrt{2} S_q[K^+\pi^0] \quad (9)$$

$$\begin{aligned}
S_-[K^+\pi^0] = -\frac{i}{2} + \frac{1}{F_0^2} \left\{ -\frac{3}{16} [A_{\text{fin}}(M_\pi^2) + 2A_{\text{fin}}(M_K^2) + A_{\text{fin}}(M_\eta^2)] - iL_9^{(0)} q^2 \right. \\
\left. +\frac{3}{16} [T_{\text{fin}}^{(1)}(q^2, M_K^2, M_\pi^2) + T_{\text{fin}}^{(1)}(q^2, M_K^2, M_\eta^2)] \right\} \quad (10)
\end{aligned}$$

$$S_-[K^+\eta] = \sqrt{3} S_-[K^+\pi^0] \quad (11)$$

$$S_-[K^0\pi^+] = \sqrt{2} S_-[K^+\pi^0] \quad , \quad (12)$$

where the particle masses M_P refer to the *one-loop renormalized masses* and the integrals are all finite and explicitly given in the Appendix.

It is worth mentioning that this result reduces to the expression known in the literature, if we restrict ourselves to *on-shell* outgoing momenta. Employing the notation of [3]

$$\langle K^+, p' | \sqrt{2} \bar{u} \gamma_\mu s | \pi^0, p \rangle = (p'_\mu + p_\mu) f_+^{K\pi}(t) + (p'_\mu - p_\mu) f_-^{K\pi}(t) \quad (13)$$

and

$$f_0^{P_1 P_2}(t) \equiv f_+^{P_1 P_2}(t) + \frac{t}{M_1^2 - M_2^2} f_-^{P_1 P_2}(t) \quad , \quad t = (p'_\mu - p_\mu)^2 \quad , \quad (14)$$

our result simplifies in the on-shell limit to (13, 14) with

$$\begin{aligned}
f_+^{K\pi}(q^2) &= f_+^{K\eta}(q^2) \\
&= 1 + \frac{i}{F_0^2} \left\{ \frac{3}{8} [T_{\text{fin}}^{(1)}(q^2, M_K^2, M_\pi^2) - A_{\text{fin}}(M_K^2) - A_{\text{fin}}(M_\pi^2)] - iq^2 L_9^{(0)} + (\pi \rightarrow \eta) \right\} \quad (15)
\end{aligned}$$

$$\begin{aligned}
f_0^{K\pi}(q^2) &= 1 + \frac{1}{F_0^2} \left\{ \frac{i}{8} \frac{q^2}{M_K^2 - M_\pi^2} [5A_{\text{fin}}(M_\pi^2) - 2A_{\text{fin}}(M_K^2) - 3A_{\text{fin}}(M_\eta^2)] + 4L_5^{(0)}q^2 \right. \\
&\quad + \frac{1}{8} [5q^2 - 2(M_K^2 + M_\pi^2) - \frac{3(M_K^2 - M_\pi^2)^2}{q^2}] \frac{1}{i} \overline{B}(q^2, M_K^2, M_\pi^2) \\
&\quad \left. + \frac{1}{24} [3q^2 - 2(M_K^2 + M_\pi^2) - \frac{(M_K^2 - M_\pi^2)^2}{q^2}] \frac{1}{i} \overline{B}(q^2, M_K^2, M_\eta^2) \right\} \quad (16)
\end{aligned}$$

$$\begin{aligned}
f_0^{K\eta}(q^2) &= 1 + \frac{1}{F_0^2} \left\{ -\frac{3i}{8} \frac{q^2}{M_K^2 - M_\eta^2} [A_{\text{fin}}(M_\pi^2) - 2A_{\text{fin}}(M_K^2) + A_{\text{fin}}(M_\eta^2)] + 4L_5^{(0)}q^2 \right. \\
&\quad + \frac{3}{8} [3q^2 - 2(M_K^2 + M_\pi^2) - \frac{(M_K^2 - M_\pi^2)^2}{q^2}] \frac{1}{i} \overline{B}(q^2, M_K^2, M_\pi^2) \\
&\quad \left. + \frac{1}{24} [-9q^2 + 2(M_K^2 + 9M_\eta^2) - \frac{9(M_K^2 - M_\eta^2)^2}{q^2}] \frac{1}{i} \overline{B}(q^2, M_K^2, M_\eta^2) \right\}. \quad (17)
\end{aligned}$$

This coincides with the result given in [3].

III. TWO-POINT FUNCTION CALCULATION

Here we give the derivation of the technical key quantity of this paper, the correlator $\langle T\{V_s V_s^\dagger\} \rangle$ between two external vector currents with the quantum numbers of a K^\pm , respectively. The convention is that V_s creates a multi-particle state with the quantum numbers of a K^+ , or annihilates a state with the quantum numbers of a K^- , i.e.

$$V_s^\mu = \bar{q}\gamma^\mu \frac{\lambda_4 + i\lambda_5}{2\sqrt{2}} q \quad (18)$$

with λ_a the standard Gell-Mann matrices and $q = (u, d, s)$. Defining the momentum-space representation of the correlator by

$$\Pi_{V,s}(q_\mu, q_\nu) = i \int d^4x e^{iq \cdot x} \langle 0 | T\{V_s^\mu(x) V_s^\nu(0)^\dagger\} | 0 \rangle, \quad (19)$$

and decomposing the latter according to

$$\Pi_{V,s}(q_\mu, q_\nu) = (q_\mu q_\nu - q^2 g_{\mu\nu}) \Pi_{V,s}^{(1)}(q^2) + q_\mu q_\nu \Pi_{V,s}^{(0)}(q^2), \quad (20)$$

the result will be given in terms of $\Pi_{V,s}^{(1)}$ and $\Pi_{V,s}^{(0)}$.

A. Calculation

For convenience we shall consider the ‘‘unitary’’, the ‘‘tadpole’’ and the ‘‘counterterm’’ contributions to $i\Pi_{V,s}$ separately, i.e. the latter is decomposed as

$$i\Pi_{V,s} = i\Pi^{\text{uni}} + i\Pi^{\text{tad}} + i\Pi^{\text{cnt}}, \quad (21)$$

where each term on the r.h.s. shall contain both the contribution at $O(p^4)$ and at $O(p^6)$ in standard chiral perturbation theory. In diagrammatic language the two-loop “unitary” contribution $i\Pi_{p^6}^{\text{uni}}$ is given by the sum of diagrams (e, f, g, h, i) in Fig. 2. The “tadpole” contribution $i\Pi_{p^6}^{\text{tad}}$ denotes the sum of diagrams (a, b, c, d), and the “counterterm” contribution $i\Pi_{p^6}^{\text{cnt}}$ is just diagram (j) in Fig. 2.

The key ingredient in the approach to the correlator $\langle T\{V_s V_s^\dagger\} \rangle$ we are describing is the observation that the “unitary piece” $i\Pi_{p^4+p^6}^{\text{uni}}$ can be computed from the renormalized strange formfactor obtained in the previous chapter. The prescription is: Contract the formfactor $S_\mu[P_1, P_2](p_1, p_2)$ with its hermitian conjugate and sum over all possible intermediate particle P_1, P_2 and momenta p_1, p_2 . In practice, several points have to be paid attention to.

First, we should mention why we defined the formfactor such that outgoing mesons carry only the square-root of the usual wavefunction renormalization factor, but neither Z nor 1: This choice allows us to proceed by splicing two of these formfactors together without having to worry again about wavefunction renormalization – the internal propagators generated in this process will automatically carry the full factor Z . The second point is that splicing the formfactor with its hermitian conjugate will yield the “eyeglass”-diagram (i) in Fig. 2 twice instead of only once. Thus one has to subtract half of the “unitary” diagram (d) in Fig. 3 from the formfactor before doing the splicing with the resulting object. In summary, the unitary piece of the correlator – which shall include the contributions both at $O(p^4)$ and at $O(p^6)$ in the chiral expansion – is constructed as

$$\begin{aligned} i\Pi_{p^4+p^6}^{\text{uni}} &= \sum_{P_1, P_2} \int \frac{d^d \ell}{(2\pi)^4} \frac{\bar{S}_\mu[P_1, P_2] \cdot \bar{S}_\nu[P_1, P_2] (i)^2}{(\ell^2 - M_1^2)((q - \ell)^2 - M_2^2)} \\ &= \sum_{P_1, P_2} \int \frac{d^d \ell}{(2\pi)^4} \left\{ \frac{(2\ell - q)_\mu (2\ell - q)_\nu (S_-^{(0)2} + 2\bar{S}_-^{(2)} \cdot S_-^{(0)} + O(p^4)) (i)^2}{(\ell^2 - M_1^2)((q - \ell)^2 - M_2^2)} \right. \\ &\quad \left. + \frac{((2\ell - q)_\mu q_\nu + q_\mu (2\ell - q)_\nu) (S_-^{(0)} \cdot \bar{S}_+^{(2)} + O(p^4)) (i)^2}{(\ell^2 - M_1^2)((q - \ell)^2 - M_2^2)} \right\}. \quad (22) \end{aligned}$$

In (22) \bar{S}_\pm denotes the “modified formfactor” in which the unitary contribution is included with a factor $\frac{1}{2}$, i.e. $\bar{S}_\pm = S_\pm - \frac{1}{2}S_\pm^{\text{uni}}$, which clearly affects only the $O(p^2)$ -contributions in $S_+[P_1, P_2] = S_+^{(2)}[P_1, P_2] + O(p^4)$ and $S_-[P_1, P_2] = S_-^{(0)}[P_1, P_2] + S_-^{(2)}[P_1, P_2] + O(p^4)$, but not $S_-^{(0)}[P_1, P_2]$. Of course \bar{S}_\pm is not renormalizable, i.e. including this factor $\frac{1}{2}$ into the formfactor already in the previous section is not an option. Note that this procedure generates an expression for $i\Pi_{p^4+p^6}^{\text{uni}}$ where the M_P refer to the *one-loop renormalized masses*.

Finally, the “unitary” piece (22) must be augmented with the “tadpole” and the “counterterm” contribution. $i\Pi_{p^4+p^6}^{\text{tad}}$ is put together from diagrams (a, b, c, d) in Fig. 2 plus the single tadpole-diagram at $O(p^4)$, i.e. diagram (b) in Fig. 1. $i\Pi_{p^4+p^6}^{\text{cnt}}$ represents the sum of diagram (j) in Fig. 2 and the single counterterm-diagram at $O(p^4)$, i.e. diagram (c) in Fig. 1. It is important to note that both $i\Pi_{p^4+p^6}^{\text{tad}}$ and $i\Pi_{p^4+p^6}^{\text{cnt}}$ happen to combine a $O(p^4)$ contribution and a $O(p^6)$ contribution in such a way that the total “tadpole” or “counterterm” contribution depends on the *one-loop renormalized masses* only.

B. Renormalization

Having added the various contributions to $S_{p^4+p^6}$ the only task left is renormalizing the result, i.e. rewriting it in such a way that it can be continued to $d = 4$ dimensions.

First we have to remind ourselves that the correlator is constructed from various elements, some of which have undergone renormalization at $O(p^4)$ already. In practice, this means that all $L_i^{(0)}$ showing up in this expression must be replaced $L_i^{(0)} \rightarrow L_i^{(0)} + L_i^{(-1)}\bar{\lambda}^{-1}$ before the so-far untouched constants get expanded according to

$$L_i \rightarrow \mu^{d-4} \cdot (L_i^{(1)}\bar{\lambda} + L_i^{(0)} + L_i^{(-1)}\bar{\lambda}^{-1} + O(\bar{\lambda}^{-2})) \quad (23)$$

$$C_j \rightarrow \mu^{2d-8} \cdot (C_j^{(2)}\bar{\lambda}^2 + C_j^{(1)}\bar{\lambda} + C_j^{(0)} + O(\bar{\lambda}^{-1})) \quad (24)$$

as is necessary in a two-loop calculation. Next, all integrals must be expanded in $1/(d-4)$, or equivalently in $\bar{\lambda}$, the latter being defined in (73) in the Appendix. For some more standard definitions in this “ $\bar{\lambda}$ -scheme” the reader is referred to [9]. An explicit calculation in this scheme, where technical aspects are presented with great care, is the analogous computation of the axial correlator to $O(p^6)$ in chiral perturbation theory [15]. A discussion of the relationship of the “ $\bar{\lambda}$ -scheme” to the $\overline{\text{MS}}$ -scheme employed in [10] is also found in [15].

The final step is checking that, after the remaining $L_i^{(1)}$ have been assigned their standard values Γ_i [2,3], there is indeed a set of numerical constants $\{C_j^{(2)}, C_j^{(1)}, L_i^{(0)}\}$ for which all contributions to the correlator with a positive power of $\bar{\lambda}$ cancel exactly. Demanding that the total contribution in proportion to $\bar{\lambda}^2$ is zero we find the constraints

$$0 = 5 - 8(4C_{38}^{(2)} + C_{91}^{(2)})F_0^2 \quad (25)$$

$$0 = 1 + 8C_{93}^{(2)}F_0^2 \quad (26)$$

$$0 = C_{61}^{(2)}F_0^2 \quad (27)$$

$$0 = C_{62}^{(2)}F_0^2 \quad (28)$$

whereas requiring the total contribution in proportion to $\bar{\lambda}$ to be zero yields

$$0 = 10L_5^{(0)} - 3(4C_{38}^{(1)} + C_{91}^{(1)})F_0^2 \quad (29)$$

$$0 = L_9^{(0)} + C_{93}^{(1)}F_0^2 \quad (30)$$

$$0 = 3(L_9^{(0)} + L_{10}^{(0)}) - 4C_{61}^{(1)}F_0^2 \quad (31)$$

$$0 = (L_9^{(0)} + L_{10}^{(0)}) - 4C_{62}^{(1)}F_0^2. \quad (32)$$

Constraints (22-29) prove consistent with what is known in the literature [9,7].

C. Results

In summary, the renormalized correlator $\langle T\{V_s V_s^\dagger\} \rangle$ between two external vector currents carrying the quantum numbers of a K^\pm respectively, is found to take the form (19, 20) with

$$\begin{aligned}
\Pi_{V,s}^{(1)} = & \left\{ -2(L_{10}^{(0)} + 2H_1^{(0)}) + \frac{3i}{4q^2} [T_{\text{fin}}^{(1)}(q^2, M_K^2, M_\pi^2) - A_{\text{fin}}(M_K^2) - A_{\text{fin}}(M_\pi^2)] \right. \\
& + \frac{3i}{4q^2} [T_{\text{fin}}^{(1)}(q^2, M_K^2, M_\eta^2) - A_{\text{fin}}(M_K^2) - A_{\text{fin}}(M_\eta^2)] \left. \right\} \\
& + \left\{ -2iL_5^{(0)} \frac{(M_K^2 - M_\pi^2)}{q^2} [3A_{\text{fin}}(M_\pi^2) - 2A_{\text{fin}}(M_K^2) - A_{\text{fin}}(M_\eta^2)] \right. \\
& + 3iL_9^{(0)} [T_{\text{fin}}^{(1)}(q^2, M_K^2, M_\pi^2) + T_{\text{fin}}^{(1)}(q^2, M_K^2, M_\eta^2)] \\
& + 3iL_{10}^{(0)} [A_{\text{fin}}(M_\pi^2) + 2A_{\text{fin}}(M_K^2) + A_{\text{fin}}(M_\eta^2)] \\
& - \frac{3}{32q^2} [-5A_{\text{fin}}(M_\pi^2)^2 + 4A_{\text{fin}}(M_\pi^2)A_{\text{fin}}(M_K^2) + 6A_{\text{fin}}(M_\pi^2)A_{\text{fin}}(M_\eta^2) \\
& \quad + 4A_{\text{fin}}(M_K^2)^2 - 12A_{\text{fin}}(M_K^2)A_{\text{fin}}(M_\eta^2) + 3A_{\text{fin}}(M_\eta^2)^2] \\
& - \frac{9}{32q^2} [T_{\text{fin}}^{(1)}(q^2, M_K^2, M_\pi^2) - A_{\text{fin}}(M_K^2) - A_{\text{fin}}(M_\pi^2) \\
& \quad + T_{\text{fin}}^{(1)}(q^2, M_K^2, M_\eta^2) - A_{\text{fin}}(M_K^2) - A_{\text{fin}}(M_\eta^2)]^2 \\
& \left. - \frac{(M_K^2 - M_\pi^2)^2}{q^2} O_V - P_V q^2 - 4M_K^2 Q_V - 4(2M_K^2 + M_\pi^2) R_V \right\} \cdot \frac{1}{F_0^2} \tag{33}
\end{aligned}$$

$$\begin{aligned}
\Pi_{V,s}^{(0)} = & \left\{ -\frac{3i}{4} \frac{(M_K^2 - M_\pi^2)^2}{q^4} \bar{B}(q^2, M_K^2, M_\pi^2) - \frac{3i}{4} \frac{(M_K^2 - M_\eta^2)^2}{q^4} \bar{B}(q^2, M_K^2, M_\eta^2) \right\} \\
& + \left\{ 2iL_5^{(0)} \frac{(M_K^2 - M_\pi^2)}{q^2} [3A_{\text{fin}}(M_\pi^2) - 2A_{\text{fin}}(M_K^2) - A_{\text{fin}}(M_\eta^2)] \right. \\
& + \frac{3}{32q^2} [-5A_{\text{fin}}(M_\pi^2)^2 + 4A_{\text{fin}}(M_\pi^2)A_{\text{fin}}(M_K^2) + 6A_{\text{fin}}(M_\pi^2)A_{\text{fin}}(M_\eta^2) \\
& \quad + 4A_{\text{fin}}(M_K^2)^2 - 12A_{\text{fin}}(M_K^2)A_{\text{fin}}(M_\eta^2) + 3A_{\text{fin}}(M_\eta^2)^2] \\
& + \kappa_{K\pi} \cdot \frac{M_K^2 - M_\pi^2}{q^2} \bar{B}(q^2, M_K^2, M_\pi^2) + \kappa_{K\eta} \cdot \frac{M_K^2 - M_\eta^2}{q^2} \bar{B}(q^2, M_K^2, M_\eta^2) \\
& \left. + \frac{(M_K^2 - M_\pi^2)^2}{q^2} O_V \right\} \cdot \frac{1}{F_0^2} \tag{34}
\end{aligned}$$

where

$$\begin{aligned}
\kappa_{K\pi} = & \frac{3}{16} [5A_{\text{fin}}(M_\pi^2) - 2A_{\text{fin}}(M_K^2) - 3A_{\text{fin}}(M_\eta^2)] - 6i(M_K^2 - M_\pi^2)L_5^{(0)} \\
& + \frac{3}{32} \left[3\frac{(M_K^2 - M_\pi^2)^2}{q^2} + 2(M_K^2 + M_\pi^2) - 5q^2 \right] \frac{(M_K^2 - M_\pi^2)}{q^2} \bar{B}(q^2, M_K^2, M_\pi^2) \\
& + \frac{3}{32} \left[-9\frac{(M_K^2 - M_\eta^2)^2}{q^2} - 2(M_K^2 + M_\pi^2) + 3q^2 \right] \frac{(M_K^2 - M_\eta^2)}{q^2} \bar{B}(q^2, M_K^2, M_\eta^2) \tag{35}
\end{aligned}$$

$$\begin{aligned}
\kappa_{K\eta} = & -\frac{9}{16} [A_{\text{fin}}(M_\pi^2) - 2A_{\text{fin}}(M_K^2) + A_{\text{fin}}(M_\eta^2)] - 6i(M_K^2 - M_\eta^2)L_5^{(0)} \\
& + \frac{3}{32} \left[-\frac{(M_K^2 - M_\pi^2)^2}{q^2} - 2(M_K^2 + M_\pi^2) + 3q^2 \right] \frac{(M_K^2 - M_\pi^2)}{q^2} \bar{B}(q^2, M_K^2, M_\pi^2) \\
& + \frac{3}{32} \left[3\frac{(M_K^2 - M_\eta^2)^2}{q^2} - \frac{2}{3}(13M_K^2 - 3M_\pi^2) + 3q^2 \right] \frac{(M_K^2 - M_\eta^2)}{q^2} \bar{B}(q^2, M_K^2, M_\eta^2) . \tag{36}
\end{aligned}$$

In (33) and (34) the contribution at $O(p^4)$ has been separated from the one at $O(p^6)$ and we have used the abbreviations

$$O_V = 4(4C_{38}^{(0)} + C_{91}^{(0)})F_0^2 - (40/3)L_5^{(-1)} \quad (37)$$

$$P_V = 4C_{93}^{(0)}F_0^2 + 4L_9^{(-1)} \quad (38)$$

$$Q_V = 4C_{61}^{(0)}F_0^2 - 3(L_9^{(-1)} + L_{10}^{(-1)}) \quad (39)$$

$$R_V = 4C_{62}^{(0)}F_0^2 - (L_9^{(-1)} + L_{10}^{(-1)}) \quad (40)$$

as these combinations of (finite parts of) $O(p^6)$ -counterterms occur quite generally [9].

While completing this paper, we received a preprint [16] where this result has been obtained independently. Up to an overall factor 2 (due to a factor $\sqrt{2}$ difference in the definition of the currents) the results agree.

IV. DISCUSSION AND LOW ENERGY THEOREM

In Sect. III we have obtained the fully renormalized finite two-loop expressions for the correlator of strangeness carrying vector currents. Here we shall first discuss the general structure of the result and point out several consistency checks which have to be satisfied on general grounds. Then we combine our result with the corresponding expressions for the isospin and hypercharge currents [9] to obtain a low energy theorem valid at $O(p^6)$.

A. Consistency checks

The correlators $\Pi_{V,s}^J$ given in Eqns. (33, 34) involve the finite functions A_{fin} , \overline{B} defined in the Appendix as well as the renormalized coupling constants $L_{5,9,10}^{(0)}$, $H_1^{(0)}$, O_V , P_V , Q_V , R_V . Note that upon taking the (1+0) component, O_V and the direct dependence on $L_5^{(0)}$ drop out (the indirect, through κ , remains). Our result satisfies the following consistency checks:

- The low energy constants and the function $A_{\text{fin}}(M_P^2)$ depend on the renormalization scale μ . Upon using Eqns. (25-32) as well as the renormalization group equations for the pertinent low energy constants [9] it can be shown that the sum of all contributions is scale independent.
- The SU(3) limit of equal quark masses provides another check: The $J = 0$ component vanishes identically, as it is in proportion to the difference of two meson masses squared. The $J = 1$ component reduces to the known results for the isospin or hypercharge component in the degenerate case. Although non-trivial, this consistency check concerns the SU(3) conserving part of the amplitude only.
- Going away from $SU(3)$, the Ademollo Gatto theorem [17] is satisfied: The $SU(3)$ breaking effect appears only in the second order in the quark masses, i.e. $\propto (m_s - \hat{m})^2$.
- Individual spin components $J = 1, 0$ exhibit poles at $q^2 = 0$. These poles must be of kinematical origin since there is no single particle state present which could generate such a singularity. Using – instead of (20) – the new decomposition

$$\Pi_{V,s}(q_\mu, q_\nu) = (q_\mu q_\nu - q^2 g_{\mu\nu}) \Pi_{V,s}^{(1+0)}(q^2) + g_{\mu\nu} q^2 \Pi_{V,s}^{(0)}(q^2), \quad (41)$$

both new components, $\Pi_{V,s}^{(1+0)}(q^2)$ and $q^2 \Pi_{V,s}^{(0)}(q^2)$ are found to be regular at $q^2 = 0$. It is thus more convenient to work with these combinations, in particular when considering dispersive representations based on analyticity assumptions.

- The explicit form (33, 34) of the vector correlator allows us to extract the corresponding spectral functions $\rho_{V,s}^{(J)} \equiv \frac{1}{\pi} \text{Im} \Pi_{V,s}^{(J)}$ for $J = 0, 1$ in a straight forward manner: The absorptive parts are contained exclusively in the functions $\bar{B}(q^2, M_1^2, M_2^2)$, i.e.

$$\text{Im} \frac{1}{i} \bar{B}(q^2, M_1^2, M_2^2) = \frac{1}{16\pi} \frac{\nu(q^2, M_1^2, M_2^2)}{q^2} \theta(q^2 - (M_1 + M_2)^2) \quad \text{with} \quad (42)$$

$$\nu(q^2, M_1^2, M_2^2) = [q^2 - (M_1 + M_2)^2]^{1/2} [q^2 - (M_1 - M_2)^2]^{1/2}. \quad (43)$$

By simply rearranging contributions one observes that the result for $J = 1$ can be expressed in terms of the on-shell vector form factor (15), viz:

$$\rho_{V,s}^{(1)} = \frac{1}{64\pi^2} \left[\frac{\nu^3(q^2, M_K^2, M_\pi^2)}{q^6} \theta(q^2 - (M_K + M_\pi)^2) + (\pi \rightarrow \eta) \right] \cdot |f_+^{K\pi}(q^2)|^2. \quad (44)$$

Likewise, but with considerable more effort, it can be shown that the $J = 0$ spectral function is given in terms of the on-shell scalar form factors (16, 17), viz:

$$\rho_{V,s}^{(0)} = \frac{3(M_K^2 - M_\pi^2)^2}{64\pi^2} \frac{\nu(q^2, M_K^2, M_\pi^2)}{q^6} \theta(q^2 - (M_K + M_\pi)^2) \cdot |f_0^{K\pi}(q^2)|^2 + (\pi \rightarrow \eta). \quad (45)$$

In deriving (44, 45) we have used the GMO relation as well as the expansion

$$|f_{+,0}^{P,Q}|^2 = 1 + 2 \text{Re} \Delta f_{+,0}^{P,Q} + O(p^4) \quad (46)$$

which follows from $f_{+,0}^{P,Q} = 1 + \text{Re} \Delta f_{+,0}^{P,Q} + i \text{Im} \Delta f_{+,0}^{P,Q}$. Eqns. (44, 45) are of course nothing else than the unitarity conditions for the absorptive parts to the order we are interested in. Phenomenologically, the XPT expressions for the $J = 1$ spectral function may (at best) be used in the immediate threshold region only, since the prominent resonance $K^*(892)$ is very close by.

The physical content of our result can be further assessed by studying the asymptotic behavior $q^2 \rightarrow \infty$ by means of the operator product expansion. Accordingly, the dispersion relations for $\Pi_{V,s}^{(1+0)}(q^2)$ and $q^2 \Pi_{V,s}^{(0)}(q^2)$ need at least one subtraction. In the chiral representation this fact is reflected by the occurrence of contact terms, e.g. those in proportion to $H_1^{(0)}$ and $C_{91}^{(0)}$. They depend on the particular way the ultraviolet divergences have been regularized. These contact terms are seen to disappear from our result upon either taking derivatives with respect to q^2 or, in the case of the $J = 1 + 0$ combination, by forming flavor breaking differences of the flavor components $\Pi_{V,f}^{(1+0)}(q^2)$ with $f \in \{3, 8, s\}$. Hence, the proper physical observables are

$$\frac{d^n}{(dq^2)^n} \Pi_{V,f}^{(1+0)}(q^2), \quad \frac{d^n}{(dq^2)^n} q^2 \Pi_{V,f}^{(0)}(q^2), \quad n = 1, 2, \dots \quad (47)$$

$$\text{and} \quad \Pi_{V,f_1}^{(1+0)}(q^2) - \Pi_{V,f_2}^{(1+0)}(q^2), \quad f_1, f_2 \in \{3, 8, s\}. \quad (48)$$

These functions depend on only two counterterm coupling constants of the $O(p^6)$ chiral Lagrangian, i.e. $P_V(\mu)$ and $Q_V(\mu)$. Since the constant $P_V(\mu)$ has already been determined to high accuracy [13], we concentrate in the following on the flavor breaking differences (48).

B. A low energy theorem

The general structure of the flavor breaking differences (48) is

$$\begin{aligned} D_{f_1 f_2}^{(1+0)}(q^2) &\equiv \Pi_{V,f_1}^{(1+0)}(q^2) - \Pi_{V,f_2}^{(1+0)}(q^2) \\ &= D_{f_1 f_2}^{1\text{-loop}}(q^2) + D_{f_1 f_2}^{2\text{-loop-cnt}}(q^2, \mu) + D_{f_1 f_2}^{\text{cnt}}(q^2, \mu). \end{aligned} \quad (49)$$

The first term in the last line of (49) denotes the total one-loop contribution. The second and third term represent the two-loop contribution which is separated into finite loop- and the finite local $O(p^6)$ counterterm pieces, respectively. Explicit expressions for these terms can be obtained from (33, 34) and Ref. [9]. Note that the $O(p^4)$ counterterms $L_{10}^{(0)}$, $H_1^{(0)}$ drop out in such differences. Hence, the only terms containing free parameters are

$$\begin{aligned} D_{3s}^{\text{cnt}}(q^2, \mu) &= 4 \frac{(M_K^2 - M_\pi^2)}{F_0^2} Q_V(\mu) \\ D_{38}^{\text{cnt}}(q^2, \mu) &= \frac{16}{3} \frac{(M_K^2 - M_\pi^2)}{F_0^2} Q_V(\mu). \end{aligned} \quad (50)$$

Consequently, there is one combination of vector-current correlators which is free of any counterterm coupling constant, viz.

$$\Delta \Pi_V(q^2) \equiv \Pi_{V,3}^{(1+0)}(q^2) + 3\Pi_{V,8}^{(1+0)}(q^2) - 4\Pi_{V,s}^{(1+0)}(q^2) = \Delta \Pi_V^{1\text{-loop}}(q^2) + \Delta \Pi_V^{2\text{-loop}}(q^2). \quad (51)$$

Eqn. (51) is a low energy theorem valid at the two-loop level. It shows that despite the many low energy constants occurring at this order of the low energy expansion it is possible to give parameter free predictions for suitably chosen combinations of observables.

The RHS of (51) is readily evaluated numerically. At $q^2 = 0$, e.g., we obtain

$$\Delta \Pi_V(0) = 0.00513 + 0.00125, \quad (52)$$

where the 1-loop and 2-loop contributions have been displayed separately. We observe a correction relative to the leading order term of $\approx 25\%$. This prediction for $\Delta \Pi_V(0)$ can be tested if the vector spectral functions $\rho_{V,f}^{(1+0)}$ are known to high accuracy. For instance, the unsubtracted dispersion relation for $\Delta \Pi_V(q^2)$ implies the chiral sum rule

$$\Delta \Pi_V(0) = \int_{4M_\pi^2}^{\infty} ds \frac{\rho_{V,3}^{(1+0)} + 3\rho_{V,8}^{(1+0)} - 4\rho_{V,s}^{(1+0)}}{s}. \quad (53)$$

Saturating the spectral functions with narrow resonances for $\rho(770)$, $\omega(782)$, $\phi(1020)$ and $K^*(892)$ gives the estimate

$$\Delta\Pi_V(0) \approx 0.039 + 0.085 - 0.121 = 0.003 . \quad (54)$$

The high degree of cancellation present in (54) clearly calls for the inclusion of finite width effects, higher resonances as well as multiparticle contributions to the spectral strengths. However, currently available data for hypercharge and strange components of the vector spectral functions do not prove accurate enough to make this test conclusive. We shall present a more detailed analysis involving the difference $\rho_{V,3}^{(1+0)} - \rho_{V,s}^{(1+0)}$ in section V below.

V. INVERSE MOMENT FINITE ENERGY SUM RULES AND DETERMINATION OF Q_V

The two-loop representation of $\Pi_{V,s}^{(1,0)}$ given in the previous sections can be combined with the isospin or hypercharge component of the vector current correlators [9,13] to form physically observable quantities. In Ref. [13] the difference between correlators of isospin and hypercharge currents was employed to estimate the finite counterterm Q_V . It has been pointed out later that isospin violating corrections have a rather large effect on the outcome of that analysis [14]. The reason is that individual components get mostly canceled such that the isospin breaking effect on the difference is enhanced. Isospin violation affects primarily the hypercharge component and is hard to be treated in a model-independent way. The aim of this section is to present an analysis based on the difference of isospin and strange components of the vector current which is less sensitive to such corrections. Thus, we shall consider the flavor breaking difference

$$\Pi(q^2) \equiv \Pi_{V,3}^{(1+0)}(q^2) - \Pi_{V,s}^{(1+0)}(q^2) , \quad (55)$$

which is free of kinematical singularities at the origin. The physical content of the XPT (chiral perturbation theory) representation of such combinations is conveniently analyzed by means of inverse moment finite energy sum rules (IMFESR) [18,19]. Unitarity and analyticity imply that the correlator (55) satisfies

$$\oint_C ds \frac{\Pi(s)w(s)}{s^{n+1}} = 0 , n = 0, 1, \dots \quad (56)$$

where C is the contour shown in Fig. 4 and $w(s)$ is a conveniently chosen weight function which is analytic inside this contour. In the following we shall consider polynomial weight functions with $w(0) = 1$. The contribution from the small circle can be computed using the XPT representation of the correlator, i.e.

$$\frac{1}{n!} \frac{d^n}{(dq^2)^n} (\Pi w)(0) = \frac{1}{2\pi i} \int_{|s|=s_0} ds \frac{\Pi(s)w(s)}{s^{n+1}} + \int_{s_{th}}^{s_0} ds \frac{\rho(s)w(s)}{s^{n+1}} , \quad n = 0, 1, \dots \quad (57)$$

with $\rho(s)$ being the spectral function of the correlator under consideration, i.e.

$$\rho(s) = \frac{1}{\pi} \text{Im} \Pi_{V,3}^{(1+0)}(s) \theta(s - 4M_\pi^2) - \frac{1}{\pi} \text{Im} \Pi_{V,s}^{(1+0)}(s) \theta(s - (M_K + M_\pi)^2) . \quad (58)$$

The first term on the right hand side of (57) can reliably be evaluated using the operator product expansion for the correlator, provided the radius of the circle, s_0 , is chosen large enough. By contrast, the second term on the RHS of (57) needs the difference of hadronic isospin and strange vector spectral functions as input. The only source of such hadronic spectral functions is provided by the tau decay data [20,11]; for this reason s_0 cannot be taken much larger than the tau mass squared.

The weight function $w(s)$ needs to satisfy 3 more conditions to make the calculation feasible. First, $w(s)$ must be chosen in such a way that the perturbative series in α_s of the leading OPE contributions is well controlled. Second, the region close to the real axis, $s = s_0$, must be suppressed since the OPE is not reliable in that region. Weight functions without this suppression substantially violate local duality. In practice, this suppression is highly welcome for reasons which relate to the third condition: As s approaches the tau mass, data become more and more uncertain. As a consequence, the integral over the hadronic spectral function is afflicted with large error bars — unless the weight function suppresses the contributions from, say, $s \geq (1.4\text{GeV})^2$. It is this point which makes the method of IMFESR superior to the conventional inverse moment chiral sum rules [13,21–23]: The high energy behavior of the weight function can be worse than what a once subtracted dispersion relation would require. Nevertheless, as long as the weight function exhibits one or two zeros at $s = s_0$, local duality is extremely well satisfied, even at scales below $s = m_\tau^2$ [24].

In the following, we shall study the IMFESR (57) for $n = 0$ using the weight-function

$$w(s) \equiv (1 - x)^3 \cdot \left(1 + x + \frac{1}{2}x^2\right), \quad x \equiv \frac{s}{s_0}. \quad (59)$$

This weight-function satisfies the conditions listed above. The factor $(1 - x)^3$ proves efficient in cutting off the region above 2GeV^2 .

Next, we specify the input needed to evaluate the inverse moment finite energy sum rule. We shall consider in turn the XPT, the OPE, and the hadronic side of the IMFESR.

A. Chiral constraints at $q^2 = 0$

The correlator at $q^2 = 0$ is obtained by straight forward evaluation of the representation of $\Pi_{V,s}^{(1+0)}$ given in section III of this paper and $\Pi_{V,3}^{(1+0)}$ as calculated in Ref. [9]. Some care has to be taken in order to show the cancellation of singular terms in the limit $q^2 \rightarrow 0$. Employing input parameters $M_\pi = 140$ MeV, $M_K = 495$ MeV, $F_0 = 93$ MeV, and, at renormalization scale $\mu = m_\rho$, $L_5^{(0)} = 0.0014 \pm 0.0005$ [25], $L_9^{(0)} = 0.00678 \pm 0.00015$, $L_{10}^{(0)} = -0.00513 \pm 0.00019$ [19] we obtain numerically

$$\Pi(0) = 0.0053 + 0.0014 + \frac{4}{F_0^2}(M_K^2 - M_\pi^2)Q_V(m_\rho^2). \quad (60)$$

The first and second term on the RHS of (60) are finite one- and two-loop terms, respectively. The counterterm coupling constant Q_V has been estimated previously, with the result

$$Q_V(\mu = m_\rho) = (3.7 \pm 2.0) 10^{-5} \quad [13] \quad (61)$$

$$Q_V(\mu = m_\rho) = (3.3 \pm 0.4) 10^{-5} \quad [14], \quad (62)$$

where the second number has been obtained with a phenomenological ansatz for the 38-component of the vector spectral function. Using the first of these values, the last term in (60) yields numerically 0.0038 ± 0.0021 , i.e. at scale $\mu = m_\rho$ it is the dominant effect of the two-loop contributions.

B. OPE of the correlator

The contributions of dimension $D = 2, 4, 6$ are known from previous work [26–28]. The $D=2$ operators are just the flavor breaking quark mass corrections:

$$\Pi(Q^2)^{D=2} = \frac{1}{Q^2} \frac{3}{4\pi^2} \left\{ m_s^2 \left[1 + \frac{7}{3} a_s + 19.9332 a_s^2 + O(a_s^3) \right] + m_s m_u \left[\frac{2}{3} a_s + O(a_s^2) \right] + O(m_u^2) \right\}, \quad (63)$$

where $Q^2 = -q^2$ denotes the Euclidean momentum, and $a_s \equiv \alpha_s(Q^2)/\pi$. Since terms in proportion to $m_s m_u$ are further suppressed by a_s , keeping the m_s^2 term only provides an excellent approximation.

Following the prescription of Ref. [29], the integration of this function over the circular contour with radius $s_0 = m_\tau^2$ is performed numerically. We use the 4-loop β - and γ -functions [30,31] for the running of mass and strong coupling constant. Weighting the correlator with $w(s)$ given in (59), we thus obtain

$$B^{D=2} \equiv \frac{1}{2\pi i} \int_{|s|=s_0} ds \frac{\Pi(s)w(s)}{s} = \frac{3}{4\pi^2} \frac{m_s^2(m_\tau^2)}{m_\tau^2} [(1.634 + 0.303 + 0.177) \pm 0.088] . \quad (64)$$

The three terms in parenthesis represent the contributions at $O(1)$, $O(a_s)$, $O(a_s^2)$ in the contour improved perturbation series. The error reflects the uncertainty due to terms of order a_s^3 , assuming a geometric growth of the series in a_s at $Q^2 = m_\tau^2$. The particular combination of moments appearing in the weight function $w(s)$ makes sure that even the resummed geometric series yields corrections not larger than the size of the a_s^3 term.

In evaluating Eqn. (64) the four-loop beta function is used, but values of a_s extracted are usually somewhat dependent on which order of perturbation theory is used. To get a handle on the uncertainty brought by the truncation in the perturbative series, we mention that the bracket in Eqn. (64) is changed into $[1.668 + 0.316 + 0.190 \pm 0.096]$ if two-loop running is used. In other words: $[2.174 \pm 0.096]$ instead of $[2.114 \pm 0.088]$ is a 3% effect.

As a result, the total error is dominated by the uncertainty of present evaluations of the strange quark mass. For a numerical evaluation we use $m_s(\mu = m_\tau) = (130 \pm 25)\text{MeV}$ [26,27,32], leading to $B^{D=2} = (8.5 \pm 3.3) 10^{-4}$. This corresponds to $\approx 16\%$ of the leading order one-loop term in (60).

The $D=4$ operators consist of two types, the quark mass corrections and terms in proportion to the quark condensates. The leading quark mass correction is in proportion to $a_s^{-1} m_s^4$. Despite the a_s^{-1} enhancement, the net contribution to the RHS of the sum rule (57) is of the order 10^{-6} , i.e. completely negligible compared to the $D=2$ contributions found above. The condensate terms read

$$\Pi(Q^2)_{\text{condensate}}^{D=4} = \frac{-1}{Q^4} \frac{m_s}{\hat{m}} \langle \hat{m} \bar{u} u \rangle \left[r_c + a_s \left(\frac{4}{3} - r_c \right) + a_s^2 \left(\frac{59}{6} - \frac{13}{3} r_c \right) \right]. \quad (65)$$

The ratio $r_c \equiv \langle \bar{s}s \rangle / \langle \bar{u}u \rangle$ lies in the range $0.7 \leq r_c \leq 1$ [26,27]. For numerical evaluation we employ leading order XPT expressions, i.e. $m_s/\hat{m} = 25.9$ and $\langle \hat{m}\bar{u}u \rangle = -F_\pi^2 M_\pi^2/2$. In this manner, the contribution to the IMFESR under consideration is also found to be of the order 10^{-6} . Hence, we can safely neglect the contributions of $D \geq 4$ operators in the OPE.

C. Hadronic spectral function

The isovector- and strange component of the vector spectral functions are constructed as follows: i) close to threshold we employ the XPT two-loop expressions given in [9] and this paper. These results depend on the low energy constants L_5, L_9 . However, due to the smallness of the spectral functions in the threshold region compared to the resonance region, uncertainties in these LECs have no detectable effect on the IMFESR (57) with $n=0$. ii) above the threshold region and up to the tau mass we employ the data as presented by the ALEPH collaboration [20,11]. We discuss this input as well as the corresponding evaluation of integrals over hadronic spectral functions for isovector- and strange component in turn:

- (a) isovector vector spectral function: the impressive set of ALEPH data [20] can be used over the whole range of integration. Data are accurate to $\approx 3\%$ for $s \leq 2\text{GeV}^2$. The region above this scale is however strongly suppressed when integrating with the weight function (59). Table 1 shows the hadronic integrals

$$B_{V,f}^{\text{had},J}(s_{\text{max}}, s_0) = \int_{s_{\text{th}}}^{s_{\text{max}}} ds \frac{\rho_f^J(s)w(s)}{s} \quad (66)$$

for various components f of the vector spectral function and different upper integration ends s_{max} . The parameter s_0 refers to the weight function (59) and is taken as large as possible, i.e. $s_0 = m_\tau^2 \simeq (1.777 \text{ GeV})^2$. The first line in Table 1 is split into three columns to illustrate the effect of not extending the integration range in (66) to its upper end s_0 , but to 1 or 2 GeV^2 only (while keeping the weight function (59) with its zero at s_0). In the isovector case, the dominant contribution to the hadronic integral stems from the region below $\sim 1 \text{ GeV}^2$, where the spectral function is still dominated by individual resonances. The error in $B_{V,3}^{\text{had}}$ is predominantly due to the correlated part of the error in the individual bins, i.e. mostly due to the uncertainty of the τ branching ratios. We are working in the isospin limit where the $J = 0$ component of the isovector vector spectral function vanishes.

- (b) strange component of the vector spectral function, $J = 1 + 0$: in a recent publication [11] the ALEPH collaboration has presented results for the strange component of vector plus axial-vector spectral functions obtained from tau decay data. Unlike in the isovector case, a full separation of vector and axial-vector components was not achieved. However, as we shall argue below, the information is sufficient to evaluate the difference of hadronic integrals we are seeking to an accuracy of $\approx 17\%$. To this end we analyze the data according to the hadronic state X in the decay $\tau \rightarrow \nu_\tau + X$:

- $X = K\pi$: the decay to the $K\pi$ final state is a pure vector current transition. The main feature of this component is the $K^*(892)$ resonance, but there is a minor

contribution associated with the interference of $K^*(1410)$. The resulting integral $B_{K\pi}^{\text{had}}$ is given in the third line of Table 1. Again, the error is primarily due to the uncertainty in the overall normalization.

- $X = K2\pi$: the final state with two pions is due to both, vector- and axial-vector transitions. As detailed in [11] the corresponding spectral function can be understood in terms of the two axial-vector resonances $K_1(1270)$, $K_1(1400)$ and the vector $K^*(1410)$. The mass resolution and statistics are not sufficient to separate the $K_1(1400)$ and $K^*(1410)$. We follow [11] and use an effective resonance instead, averaging the parameters of the two states. The vector part is then estimated by fitting $\rho_{v,s}^{(1)} + \rho_{a,s}^{(1)}$ to two resonances with masses $m_1 = 1.270$ GeV, $m_2 = 1.405$ GeV. Switching off the axial $K_1(1270)$ yields an estimate for the contribution from the resonances at $s = (1.4 \text{ GeV})^2$. Half of the remaining spectral strength is assumed to be vector, with an estimated error of ≈ 50 %. This procedure is roughly consistent with the vector- axial-vector separation of branching ratios shown in Table 7 of Ref. [11]. The contribution to the hadronic integral $B_{K2\pi}^{\text{had}}$ is roughly 7 % of the $K\pi$ component, see Table 1.
- $X = K\eta$ and $K3\pi$: this component has not been separated into vector- and axial-vector contribution. However, the spectral strength associated with these final states is relevant only above $s \approx (1.3 \text{ GeV})^2$. Due to the suppression of this energy region by the weight function, the net contribution to the hadronic integral is small. We assign half of this component to the vector current and employ the rest of the spectral strength as an estimate for the error.
- $X = Kn\pi$ for $n \geq 4$: these components are small and non-zero only above $s = 2 \text{ GeV}^2$. For this reason they can safely be neglected.

Again, the different columns in Table 1 illustrate the effect of not extending the integration range in (66) to its upper end s_0 , but to 1 or 2 GeV^2 only (while keeping the weight function (59) with its zero at s_0). The contributions to the strange vector spectral function are not dominated by the low-energy part as impressively as the non-strange part, but still the integrals are almost saturated at $\sim 1 \text{ GeV}^2$.

- (c) strange component of the vector spectral function, $J = 0$: the main contribution to the exclusive $J = 0$ component is provided by production of the scalar resonance $K_0^*(1430)$, which decays almost exclusively to the $K\pi$ final state [11]. In order to obtain an estimate for this component we use an Omnès representation as given in Ref. [28]. Employing also input parameters as detailed in [28] yields the integrals as shown in Table 1. The error is an educated guess of the various uncertainties entering the Omnès representation. This effect is already accounted for in the $K\pi$ component and should not be included when summing the strange contributions to $B_{V,s}^{\text{had}}$.

The hadronic integrals summed over the strange components of the vector spectral functions is given in the third to last line of Table 1. Subtracting this result from the hadronic integral over the isovector component and adding errors in quadrature we finally obtain

$$B_{V,3}^{\text{had}} - B_{V,s}^{\text{had}} = 0.0087 \pm 0.0013 . \quad (67)$$

Individual flavor components thus have canceled to $\approx 60\%$. The error stems mostly from the error on the $K\pi$ -component of the strangeness carrying vector spectral function, but the error on the $K2\pi$ -component is non-negligible as well.

The final step is plugging the results of Eqns. (60, 64, 67) into the IMFESR (57) for $n = 0$, which yields

$$Q_V(\mu = m_\rho) = (2.8 \pm 1.3) \cdot 10^{-5}. \quad (68)$$

This result is consistent with the determinations (61, 62), but with the advantage of being both, relatively precise and free of model assumptions.

The variation of Q_V with renormalization scale μ is known [9]:

$$Q_V(\mu) - Q_V(\mu_0) = -\frac{3}{32\pi^2} \left(L_9^{(0)}(M_\rho) + L_{10}^{(0)}(M_\rho) \right) \ln \frac{\mu^2}{\mu_0^2}. \quad (69)$$

Q_V is thus strongly varying with scale. Explicitly we obtain e.g. $Q_V(500\text{MeV}) = (4.2 \pm 1.4)10^{-5}$ and $Q_V(1\text{GeV}) = (2.0 \pm 1.4)10^{-5}$. However, the method employed here deals with RG-invariant quantities, and the variation with scale does not lead to any further ambiguities in the determination of Q_V . We also note that the coupling Q_V is the same in both, the $\bar{\lambda}$ -subtraction scheme used here and the $\bar{\text{M}}\text{S}$ -scheme [15].

In our determination, s_0 was chosen as large as possible by having it equal to m_τ^2 . Of course one may ask whether the total result is stable under a variation of the radius of the outer circle in Fig. 4. Since there are no data from τ -decays with $s > m_\tau^2$, the only alternative is a radius which is smaller than our choice $s_0 = m_\tau^2$. Concerning the contribution from the hadronic spectral integral, there is a clear numerical answer to this question. Repeating our calculation, now replacing [both, in the upper boundary of the integral (66) and in the weight function (59)] $s_0 = (1.777 \text{ GeV})^2$ by $(1.555 \text{ GeV})^2$ and $(1.333 \text{ GeV})^2$, we find the values collected in Table 2. As one can see, the total hadronic spectral integral ($3 - s$ component) is extremely stable under this shift. On the other hand any numerical statement about the shift in the contribution from the outer circle is somewhat questionable. Lowering the radius in the integral (64) to $|s| = s_1 = (1.555 \text{ GeV})^2$ results in the bracket in the r.h.s. being replaced by $[1.570 + 0.302 + 0.180 \pm 0.090]$. Going further down to a radius as small as $|s| = s_2 = (1.333 \text{ GeV})^2$ gives a bracket which takes the value $[1.474 + 0.296 + 0.181 \pm 0.093]$. The corresponding shift in $B^{D=2}$ is small compared to the error brought by the uncertainty in present evaluations of the strange quark mass. Hence, the contribution from the outer circle seems to be insensitive to the precise value of the radius too. The real problem, however, is that the expansion in contributions at different orders in the OPE breaks down at s -values substantially below 4GeV^2 . In this respect choosing $s_0 = m_\tau^2$ amounts to stretching the validity of the perturbative expansion to the very end. All one can say is that our result is stable under *small* variations of the outer radius in Fig. 4.

Regarding the error, it is clear that a more accurate determination of both the strange and the non-strange τ branching ratios as well as a more accurate measurement of the $K\pi$ -component of the vector spectral function below $s = (1.4 \text{ GeV})^2$, in particular in the $K^*(892)$ region, will transform into a more precise determination Q_V . As for the $K2\pi$ component, a full separation into V- and A- part would further diminish the error.

Our final value for Q_V supports the claim by Maltman and Wolfe [14] that isospin breaking effects tend to reduce the estimate (61).

VI. CONCLUSIONS

We have calculated the two-point function of strangeness carrying vector currents to two-loop standard chiral perturbation theory, in the isospin limit. Our fully renormalized finite result passes several consistency checks: The sum of all contributions does not depend on the renormalization scale μ . In the $SU(3)$ limit of equal quark masses it reduces to the known results for the two-point functions of isospin and hypercharge currents. The $SU(3)$ breaking part satisfies the constraint imposed by the Ademollo Gatto theorem. Furthermore, kinematical singularities at zero momentum transfer present in the spin 0 and spin 1 components are shown to be absent if a convenient and well-known decomposition is chosen. Last but not least, the imaginary parts of the correlators for spin 0 and 1 obey the unitarity-conditions along the two-particle cut implying that they can be expressed in terms of the vector and scalar meson form-factors.

The calculated correlators $\Pi_{V,s}^{(J)}$ for $J=0,1$ depend on several low energy constants (LEC). Two of these constants are related to contact terms. In physical observables, which do not depend on contact terms, only two low energy constants of the $O(p^6)$ chiral Lagrangian remain, i.e. P_V and Q_V . We have shown that at $O(p^6)$ in the low energy expansion the combination $(\Pi_{V,3}^{(1+0)} + 3\Pi_{V,8}^{(1+0)} - 4\Pi_{V,s}^{(1+0)})(q^2)$ is free of any unknown LEC and consequently predicted in terms of pseudoscalar meson masses and decay constants only. This low energy theorem (LET) can be tested once the vector spectral functions $\rho_{V,3}$, $\rho_{V,8}$ and $\rho_{V,s}$ are known to high accuracy. Presently, data are not accurate enough to make such a test conclusive, but the situation might change within a couple of years.

Finally we have presented a determination of the low energy constant Q_V based on an inverse moment finite energy sum rule. The sum rule employs the difference of isospin and strange components of vector spectral functions and is therefore expected to be less sensitive to isospin breaking effects than previous attempts. Our analysis is based on the recently released ALEPH data of τ -decays into strangeness carrying final states. Presently, the error bars on the data are still too large to make the uncertainty of our first-principle based Q_V determination smaller than the statistical error of previous model-based calculations. However, the fact that the main uncertainty stems from the dominant decay channel means that our hope for more precise experimental data might be realistic. The very same experimental effort would also be welcome in view of the low energy theorem discussed above.

Acknowledgments

We are grateful to G. Colangelo, J. Gasser and K. Maltman for illuminating discussions and to S. Chen for providing us with data on the strange component of the vector spectral function. This work is supported in part by U.S. Department of Energy grant DE-FG03-96ER40956 and the EEC-TMR Program, Contract No CT98-0169. Both authors acknowledge support from the Swiss National Science Foundation.

APPENDIX: SURVEY OF ONE-LOOP INTEGRALS

Here we give a survey of the integrals occurring in the computation of the formfactor and the desired correlator. We shall keep d arbitrary and isolate the divergences near $d \rightarrow 4$.

The simplest quantity is the scalar integral

$$A(m^2) = \int \frac{d^d \ell}{(2\pi)^d} \frac{1}{\ell^2 - m^2} \quad (70)$$

which, by standard means, is evaluated to give

$$A(m^2) = \frac{-i}{(4\pi)^{d/2}} \Gamma(1 - \frac{d}{2}) (m^2)^{(d/2-1)}. \quad (71)$$

From this expression it is found to split

$$A(m^2) = -2i m^2 \mu^{(d-4)} \bar{\lambda} + A_{\text{fin}}(m^2) \quad \text{with} \quad (72)$$

$$\bar{\lambda} = \frac{1}{16\pi^2} \left(\frac{1}{d-4} - \frac{1}{2}(\log(4\pi) - \gamma + 1) \right) \quad (73)$$

$$A_{\text{fin}}(m^2) = \mu^{(d-4)} \left(-\frac{im^2}{16\pi^2} \log\left(\frac{m^2}{\mu^2}\right) + \dots \right) \quad (74)$$

where (74) is the part of A which stays finite under $d \rightarrow 4$ in this so-called $\bar{\lambda}$ -scheme. Each of the contributions in (72) depends on the artificial scale μ and the prefactor $\mu^{(d-4)}$ is introduced in order to give them the appropriate mass dimension in d space-time dimensions.

We shall define

$$B(q^2, m_1^2, m_2^2) = \int \frac{d^d \ell}{(2\pi)^d} \frac{1}{(\ell^2 - m_1^2) ((\ell - q)^2 - m_2^2)} \quad (75)$$

$$B_\mu(q, m_1^2, m_2^2) = \int \frac{d^d \ell}{(2\pi)^d} \frac{q_\mu}{(\ell^2 - m_1^2) ((\ell - q)^2 - m_2^2)} \quad (76)$$

$$B_{\mu\nu}(q, m_1^2, m_2^2) = \int \frac{d^d \ell}{(2\pi)^d} \frac{q_\mu q_\nu}{(\ell^2 - m_1^2) ((\ell - q)^2 - m_2^2)} \quad (77)$$

as well as the finite quantity

$$\bar{B}(q^2, m_1^2, m_2^2) = B(q^2, m_1^2, m_2^2) - B(0, m_1^2, m_2^2) \quad (78)$$

which obviously satisfies $\bar{B}(0, m_1^2, m_2^2) = 0$. Then the exact relations (in d dimensions)

$$B(0, m^2, m^2) = \frac{(d-2)}{2} \frac{A(m^2)}{m^2} \quad (79)$$

$$B(0, m_1^2, m_2^2) = \frac{A(m_1^2) - A(m_2^2)}{m_1^2 - m_2^2} \quad (80)$$

follow by taking a derivative in (70, 71) and by partial fraction decomposition in (75). Invoking covariance, B_μ and $B_{\mu\nu}$ in Eqns. (76, 77) may be decomposed as

$$B_\mu(q, m_1^2, m_2^2) = q_\mu B_1(q^2, m_1^2, m_2^2) \quad (81)$$

$$B_{\mu\nu}(q, m_1^2, m_2^2) = q_\mu q_\nu B_{21}(q^2, m_1^2, m_2^2) + g_{\mu\nu} B_{22}(q^2, m_1^2, m_2^2). \quad (82)$$

Considering $q_\mu B_\mu$ one finds

$$B_1(q^2, m_1^2, m_2^2) = \frac{1}{2} \left(1 + \frac{m_1^2 - m_2^2}{q^2}\right) B(q^2, m_1^2, m_2^2) - \frac{(A(m_1^2) - A(m_2^2))}{2q^2} \quad (83)$$

$$= \frac{1}{2} \left(1 + \frac{m_1^2 - m_2^2}{q^2}\right) \bar{B}(q^2, m_1^2, m_2^2) + \frac{(A(m_1^2) - A(m_2^2))}{2(m_1^2 - m_2^2)} \quad (84)$$

where in (84) one would have to use Eqns. (79, 80) for performing the equal mass limit. Considering $q_\mu B_{\mu\nu}$ and $g_{\mu\nu} B_{\mu\nu}$ one finds

$$(d-1) B_{21} = \frac{d}{2} \left(1 + \frac{m_1^2 - m_2^2}{q^2}\right) B_1 - \frac{m_1^2}{q^2} B + \frac{d-2}{2q^2} A(m_2^2) \quad (85)$$

$$= \frac{d(q^2 + m_1^2 - m_2^2)^2 - 4q^2 m_1^2}{4q^2} \bar{B} - \frac{(4-d)m_1^2 - d(q^2 - m_2^2)}{4(m_1^2 - m_2^2)q^2} A(m_1^2) - \frac{d(q^2 - m_1^2) - (4-d)m_2^2}{4(m_1^2 - m_2^2)q^2} A(m_2^2) \quad (86)$$

$$(d-1) B_{22} = -\frac{1}{2}(q^2 + m_1^2 - m_2^2) B_1 + m_1^2 B - \frac{1}{2} A(m_2^2) \quad (87)$$

$$= -\frac{q^4 - 2q^2(m_1^2 + m_2^2) + (m_1^2 - m_2^2)^2}{4q^2} \bar{B} - \frac{q^2 - 3m_1^2 - m_2^2}{4(m_1^2 - m_2^2)} A(m_1^2) + \frac{q^2 - m_1^2 - 3m_2^2}{4(m_1^2 - m_2^2)} A(m_2^2) \quad (88)$$

where in (86) and (88) one would have to use Eqns. (79, 80) for performing the equal mass limit. A combination frequently occurring in loop integrals is

$$T_{\mu\nu}(q, m_1^2, m_2^2) = 4B_{\mu\nu} - 2q_\mu B_\nu - 2q_\nu B_\mu + q_\mu q_\nu B \quad (89)$$

$$= g_{\mu\nu} 4B_{22} + q_\mu q_\nu (4B_{21} - 4B_1 + B) \quad (90)$$

$$= P_{\mu\nu}^{(0)} \cdot (4B_{22} + (4B_{21} - 4B_1 + B) q^2) + P_{\mu\nu}^{(1)} \cdot (4B_{22}) \quad (91)$$

where, in the last line, we have introduced the projection operators

$$P_{\mu\nu}^{(0)} = \frac{q_\mu q_\nu}{q^2} \quad \text{and} \quad P_{\mu\nu}^{(1)} = g_{\mu\nu} - \frac{q_\mu q_\nu}{q^2}. \quad (92)$$

Denoting $T^{(0)} = 4B_{22} + (4B_{21} - 4B_1 + B) q^2$ and $T^{(1)} = 4B_{22}$ the spin-0 and spin-1 components, respectively, and using the decompositions (84, 86, 88) along with (78, 79, 80) these two pieces are found to split up into divergent and finite parts

$$T_{\text{div}}^{(0)}(q^2, m_1^2, m_2^2) = -2i (m_1^2 + m_2^2) \mu^{(d-4)} \bar{\lambda} \quad (93)$$

$$T_{\text{fin}}^{(0)}(q^2, m_1^2, m_2^2) = \frac{(m_1^2 - m_2^2)^2}{q^2} \bar{B}(q^2, m_1^2, m_2^2) + A_{\text{fin}}(m_1^2) + A_{\text{fin}}(m_2^2) \quad (94)$$

$$T_{\text{div}}^{(1)}(q^2, m_1^2, m_2^2) = \frac{2i}{3} (q^2 - 3(m_1^2 + m_2^2)) \mu^{(d-4)} \bar{\lambda} \quad (95)$$

$$\begin{aligned}
T_{\text{fin}}^{(1)}(q^2, m_1^2, m_2^2) = & -\frac{1}{3} \left\{ \frac{q^4 - 2q^2(m_1^2 + m_2^2) + (m_1^2 - m_2^2)^2}{q^2} \overline{B}(q^2, m_1^2, m_2^2) \right. \\
& + \frac{q^2 - 3m_1^2 - m_2^2}{m_1^2 - m_2^2} A_{\text{fin}}(m_1^2) - \frac{q^2 - m_1^2 - 3m_2^2}{m_1^2 - m_2^2} A_{\text{fin}}(m_2^2) \\
& \left. + \frac{i}{24\pi^2} (q^2 - 3(m_1^2 + m_2^2)) \right\}, \tag{96}
\end{aligned}$$

where terms contributing to $O(d-4)$ have been dropped and where the equal-mass limit is trivial for every quantity but $T_{\text{fin}}^{(1)}$, for which it takes the form

$$T_{\text{fin}}^{(1)}(q^2, m^2, m^2) = -\frac{1}{3} \left\{ (q^2 - 4m^2) \overline{B}(q^2, m^2, m^2) + (q^2 - 6m^2) \frac{A_{\text{fin}}(m^2)}{m^2} - \frac{iq^2}{48\pi^2} \right\}. \tag{97}$$

TABLES

$s_{\text{max}} (\leq s_0) :$	1GeV ²	2GeV ²	$s_0 = (1.777 \text{ GeV})^2$
3-component, J=(1)=(1+0)	0.0240 ± 0.0005	0.0254 ± 0.0005	0.0257 ± 0.0005
$K\pi$ -component	0.0146 ± 0.0009	0.0155 ± 0.0010	0.0155 ± 0.0010
$K2\pi$ -component	0.0000 ± 0.0002	0.0008 ± 0.0004	0.0011 ± 0.0006
$K\eta$ - and $K3\pi$ -component	0.0000 ± 0.0002	0.0003 ± 0.0003	0.0004 ± 0.0004
sum s-component, J=(1+0)	0.0146 ± 0.0009	0.0166 ± 0.0011	0.0170 ± 0.0012
3-s, J=(1+0)			0.0087 ± 0.0013
s-component, J=(0)			0.0011 ± 0.0004

Table I: *Hadronic integrals* $B_{V,f}^{\text{had},J}(s_{\text{max}}, s_0)$ as defined in (66) for various components f of the total vector spectral function $\rho_{V,f}^J$ as defined in Eqn. (58). Weight function is (59) with $s_0 = m_\tau^2 = (1.777 \text{ GeV})^2$.

	$s_{\text{max}} = s_2 = (1.333\text{GeV})^2$	$s_{\text{max}} = s_1 = (1.555\text{GeV})^2$
3-component, J=(1)=(1+0)	0.0160 ± 0.0004	0.0213 ± 0.0005
$K\pi$ -component	0.0073 ± 0.0005	0.0119 ± 0.0008
$K2\pi$ -component	0.0000 ± 0.0001	0.0003 ± 0.0003
$K\eta$ - and $K3\pi$ -component	0.0000 ± 0.0001	0.0001 ± 0.0002
sum s-component, J=(1+0)	0.0073 ± 0.0005	0.0123 ± 0.0009
3-s, J=(1+0)	0.0087 ± 0.0006	0.0090 ± 0.0010
s-component, J=(0)	0.0003 ± 0.0001	0.0007 ± 0.0003

Table II: *Hadronic integrals* $B_{V,f}^{\text{had},J}(s_2, s_2)$ as defined in (66) for various components f of the total vector spectral function $\rho_{V,f}^J$ as defined in Eqn. (58). Weight function is (59) with $s_0 \rightarrow s_1 = (1.555 \text{ GeV})^2$ and $s_0 \rightarrow s_2 = (1.333 \text{ GeV})^2$, respectively. Either one of the two columns corresponds to the rightmost column in Table I.

FIGURES

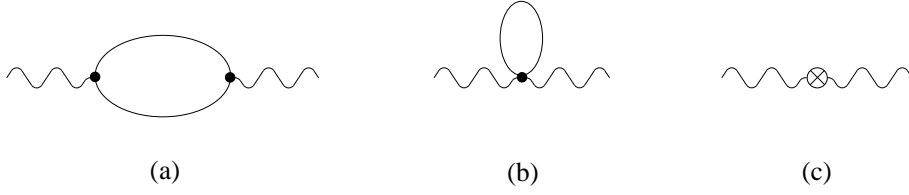


FIG. 1. One-loop Feynman graphs for $\Pi_{V,s}$. Dots and crossed circles denote vertices from the lagrangian of order p^2 and p^4 respectively. Wavy lines are external vector currents, straight lines denote Goldstone boson propagators.

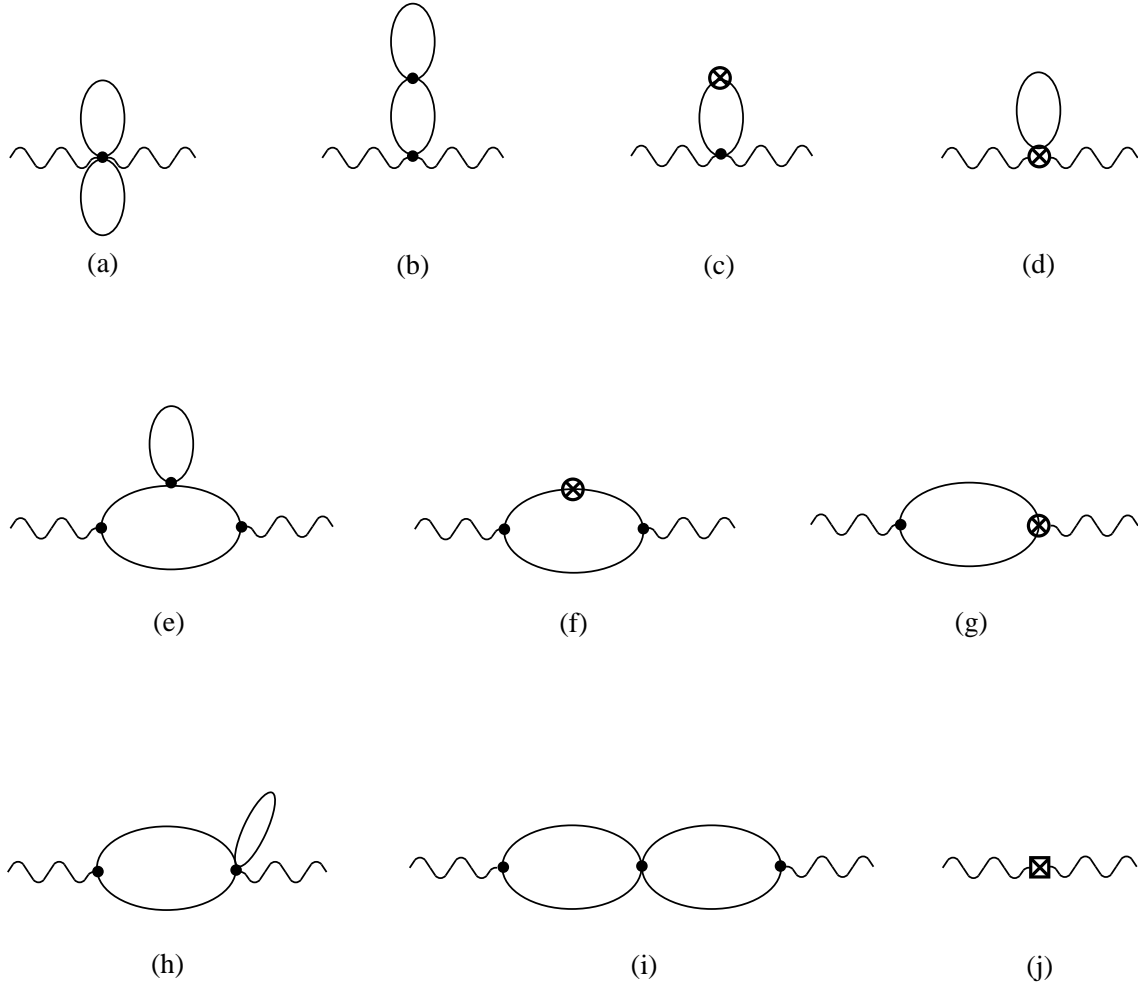


FIG. 2. Two-loop Feynman graphs for $\Pi_{V,s}$. In addition to the conventions as in Fig. 1, the crossed square denotes a vertex from the lagrangian of order p^6 . Diagrams (g) and (h) shall comprise the corresponding modification to the incoming vector-vertex as well.

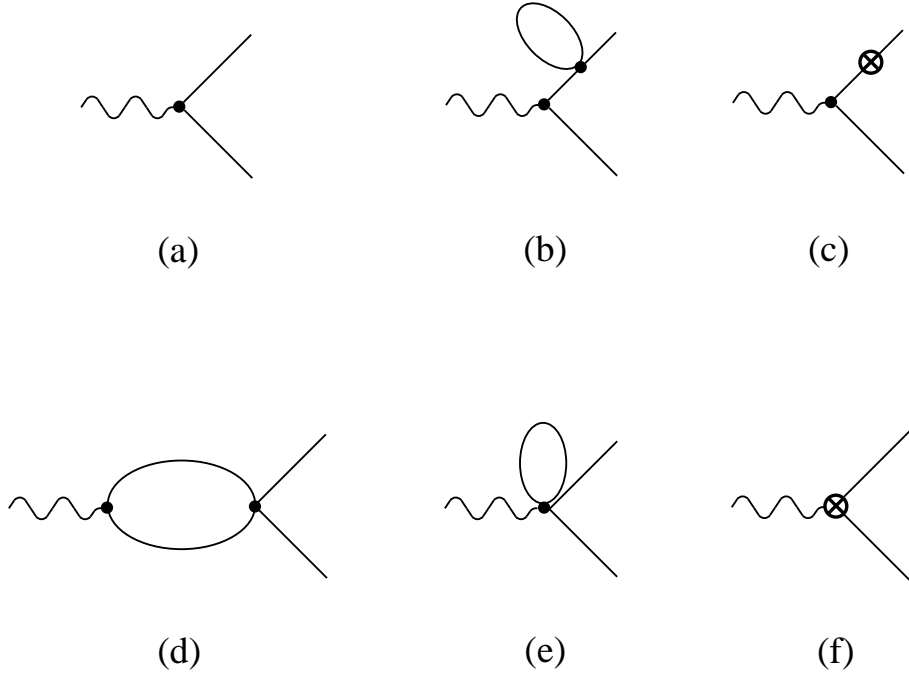


FIG. 3. Feynman graphs for meson form factors at one-loop. The partial wavefunction renormalization convention used in the calculation affects the weight of diagrams (b, c) – see text.

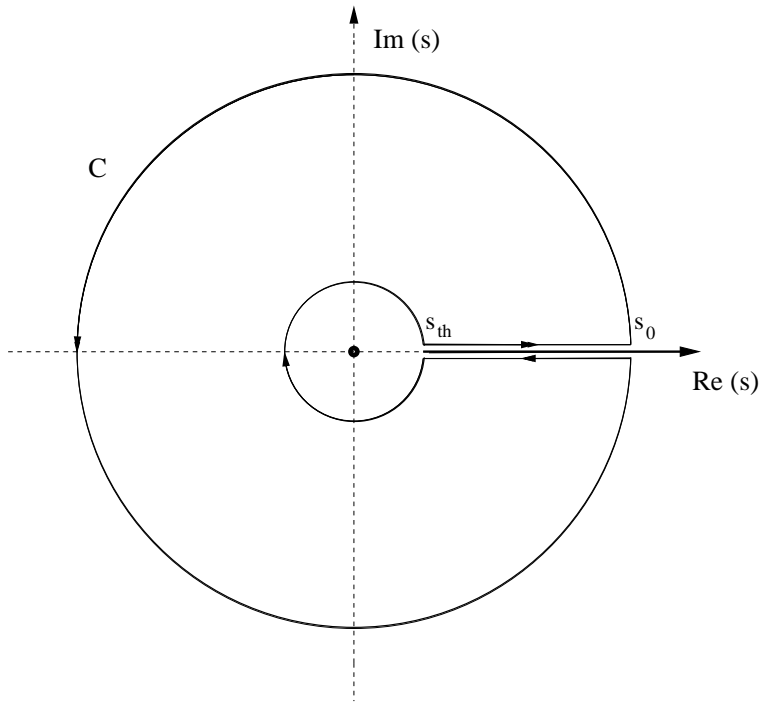


FIG. 4. Integration contour for the inverse moment finite energy sum rule (56). The cut on the real axis starts at s_{th} and extends to infinity. The dot at the origin indicates possible poles in the case of inverse moment finite energy sum rules.

REFERENCES

- [1] S. Weinberg, *Physica* **A96**, 327 (1979).
- [2] J. Gasser and H. Leutwyler, *Ann. Phys.* **158** (1984), 142.
- [3] J. Gasser and H. Leutwyler, *Nucl. Phys.* **B 250** (1985), 465.
- [4] H. Leutwyler, *Ann. Phys.* **235** (1994), 165.
- [5] J. Bijnens, G. Colangelo and G. Ecker, *J. High Energy Phys.* **9902** (1999), 020.
- [6] H.W. Fearing and S. Scherer, *Phys. Rev.* **D 53** (1996), 315.
- [7] J. Bijnens, G. Colangelo, G. Ecker, hep-ph/9907333.
- [8] S. Bellucci, J. Gasser and M.E. Sainio, *Nucl. Phys.* **B 423** (1994), 80 and *Nucl. Phys.* **B 431** (1994), 413 (Erratum); B. Holdom, R. Lewis and R.R. Mendel, *Z. Phys.* **C 63** (1994), 71; K. Maltman, *Phys. Rev.* **D 53** (1996), 2573; U. Bürgi, *Phys. Lett.* **B 377** (1996), 147 and *Nucl. Phys.* **B 479** (1996), 392; M. Jetter, *Nucl. Phys.* **B 459** (1996), 283; J. Bijnens et. al., *Phys. Lett.* **B 374** (1996), 210; J. Bijnens and P. Talavera, *Nucl. Phys.* **B 489** (1997), 387; P. Post and K. Schilcher, *Phys. Rev. Lett.* **79** (1997), 4088; J. Bijnens, G. Colangelo and P. Talavera, *J. High Energy Phys.* **05** (1998), 014.
- [9] E. Golowich and J. Kambor, *Nucl. Phys.* **B 447** (1995), 373.
- [10] J. Bijnens et. al., *Nucl. Phys.* **B 508** (1997), 263 and *Nucl. Phys.* **B 517** (1998), 639 (Erratum).
- [11] R. Barate et al. (ALEPH Collaboration), hep-ex/9903015, *Eur. Phys. J.* **C 11** (1999), 599.
- [12] S. Narison, hep-ph/9905264.
- [13] E. Golowich and J. Kambor, *Phys. Rev.* **D 53** (1996), 2651.
- [14] K. Maltman and C.E. Wolfe, *Phys. Rev.* **D 59** (1999), 096003.
- [15] E. Golowich and J. Kambor, *Phys. Rev.* **D 58** (1998), 036004.
- [16] G. Amoros, J. Bijnens and P. Talavera, hep-ph/9907264.
- [17] M. Ademollo and R. Gatto, *Phys. Rev. Lett.* **13** (1964), 264; R.E. Behrends and A. Sirlin, *Phys. Rev. Lett.* **4** (1960), 186.
- [18] E.G. Floratos, S. Narison and E. de Rafael, *Nucl. Phys.* **B 155** (1979), 115; R.A. Bertlmann, G. Launer and E. de Rafael, *Nucl. Phys.* **B 250** (1985), 61.
- [19] M. Davier, L. Girlanda, A. Hoecker and J. Stern, *Phys. Rev.* **D 58** (1998), 096014.
- [20] R. Barate et al. (ALEPH Collaboration), *Z. Phys.* **C 76** (1997), 15.
- [21] J.F. Donoghue and E. Golowich, *Phys. Rev.* **D 49** (1994), 1513.
- [22] E. Golowich and J. Kambor, *Phys. Rev. Lett.* **79** (1997), 4092.
- [23] E. Golowich and J. Kambor, *Phys. Lett.* **B 421** (1998), 319.
- [24] K. Maltman, *Phys. Lett.* **B 440** (1998), 367.
- [25] G. Ecker, in “Chiral Dynamics: Theory and Experiment”, Proc. of the Workshop at MIT, A.M. Bernstein and B.R. Holstein, Eds., July 1994, Springer-Verlag (Berlin 1995).
- [26] M. Jamin and M. Münz, *Z. Phys.* **C 66** (1995), 633.
- [27] K.G. Chetyrkin, D. Pirjol and K. Schilcher, *Phys. Lett.* **B 404** (1997), 337.
- [28] P. Colangelo, F. De Fazio, G. Nardulli and N. Paver, *Phys. Lett.* **B 408** (1997), 340.
- [29] F. Le Diberder and A. Pich, *Phys. Lett.* **B 289** (1992), 165.
- [30] T. van Ritbergen, J.A.M. Vermaseren and S.A. Larin, *Phys. Lett.* **B 400** (1997), 379.
- [31] K.G. Chetyrkin, *Phys. Lett.* **B 404** (1997), 161.
- [32] K. Maltman, hep-ph/9904370, *Phys. Lett.* **B 462** (1999), 195.